Impact of antisymmetric contributions to signal multipoles in the measurement of black-hole spins

Panagiota Kolitsidou,[1,2] Jonathan E. Thompson,[3,2] and Mark Hannam[2]

[1]*School of Physics and Astronomy and Institute for Gravitational Wave Astronomy, University of Birmingham, Edgbaston, Birmingham B15 2TT, United Kingdom*

[2]*School of Physics and Astronomy, Cardiff University, Cardiff CF24 3AA, United Kingdom*

[3]*Theoretical Astrophysics Group, California Institute of Technology, Pasadena, California 91125, USA*

(Received 2 February 2024; accepted 8 November 2024; published 21 January 2025)

Many current models for the gravitational-wave signal from precessing black-hole binaries neglect an asymmetry in the $\pm m$ multipoles. The asymmetry is weak, but is responsible for out-of-plane recoil, which for the final black hole can be several thousand km/s. In this work we show that the multipole asymmetry is also necessary to accurately measure the black-hole spins. We consider synthetic signals calculated from the numerical relativity surrogate model NRSur7dq4, which includes the multipole asymmetry, and measure the signal parameters using two versions of the same model, one with and one without the multipole asymmetry included. We find that in high signal-to-noise-ratio observations where the spin magnitude and direction can in principle be measured accurately, neglecting the multipole asymmetry can result in biased measurements of these quantities. Measurements of the black-hole masses and the standard aligned-spin combination $\chi_{\rm eff}$ are not in general strongly affected. As an illustration of the impact of the multipole asymmetry on a real signal we consider the LIGO-Virgo-KAGRA observation GW200129_065458, and find that the inclusion of the multipole asymmetry is necessary to identify the binary as unequal mass and a high in-plane spin in the primary.

DOI: 10.1103/PhysRevD.111.024050

I. INTRODUCTION

Gravitational-wave (GW) observations of binary black holes (BBHs) have begun to uncover the astrophysical population of stellar-mass black holes (BHs) in the Universe [1,2]. The distribution of BH masses and their angular momenta (spins) also provides hints of the dominant binary formation mechanisms (Refs. [1–4] and references therein). In the ∼80 BBH observations in the first three LIGO-Virgo-KAGRA (LVK) [5–7] observing runs from 2015 to 2020, most signals have been too weak to allow measurements of the full spin information for both BHs in a binary, and astrophysical inference has relied primarily on the distribution of black-hole masses, and the most accurately measured combination of the two spins, a mass-weighted sum of the spin components aligned with the binary's orbital angular momentum, $\chi_{\rm eff}$ [8]. As detector sensitivities improve, and we accrue more observations, more signals will be loud enough for us to also measure the in-plane spin components, and to distinguish both spins.

Accurate spin measurements will also require sufficiently accurate theoretical signal models. All current models rely on a combination of approximate semianalytic calculations and/or numerical solutions of Einstein's equations, and their physical fidelity is limited by the accuracy of each of these inputs, and also physical approximations used to simplify the model construction. As we will discuss, one simplification effectively neglects an asymmetry in the $\pm m$ spherical-harmonic multipoles. The purpose of this work is to study the impact of that asymmetry on the measurement of BH properties, in particular the spins.

The BHs in a binary are characterized by their masses, m_1 and m_2 (the total mass is $M = m_1 + m_2$), and their spin angular momenta, $\mathbf{S}_1$ and $\mathbf{S}_2$, which are usually expressed as the dimensionless vectors $\boldsymbol{\chi}_i = \boldsymbol{a}_i/m_i = \mathbf{S}_i/m_i^2$. When $\boldsymbol{\chi}_i$ are aligned with the binary's orbital angular momentum $\hat{\mathbf{L}}$, the orbital plane and spin directions remain constant. For these "aligned-spin" or "nonprecessing" binaries, if the gravitational-wave signal is decomposed in the spin-weighted spherical harmonics with weight $s = -2$,

$$h(t,\theta,\phi) = \sum_{\ell,m} h_{\ell m}(t)\,{}^{-2}Y_{\ell m}(\theta,\phi), \tag{1}$$

the multipoles obey the reflection symmetry,

$$h_{\ell m} = (-1)^{\ell} h^*_{\ell -m}. \quad (2)$$

This symmetry simplifies the construction of aligned-spin waveform models: we need only model the $+m$ multipoles and can then directly calculate the $-m$ multipoles from symmetry.

When the spins are misaligned with the orbital angular momentum, the binary's orbital plane and spins precess [9,10]. This complicates the modeling process, and many models make use of a convenient approximation: during the inspiral we can consider the signal from a coprecessing frame that tracks the precession of the orbital angular momentum. All current precessing-binary models employ the idea of a coprecessing frame. In this frame the signal equals, to a good approximation, that from a nonprecessing system with the same aligned-spin components $\chi_i \cdot \hat{\mathbf{L}}$ [11]. One way to produce an approximate precessing-binary model, then, is to take a nonprecessing-binary model and apply a time-dependent rotation to introduce any precession dynamics. This motivates the construction of the coprecessing-frame signal in all of the PHENOM and SEOBNR models used in LVK analyses to date [12–21].

In all of these models the coprecessing-frame model includes in-plane-spin contributions, but retains the basic structure of the aligned-spin multipoles. In particular, the coprecessing-frame multipoles retain the symmetry in Eq. (2), which no longer holds for precessing binaries. (As noted in Ref. [22], rotations cannot restore this symmetry.) The current PHENOM and SEOBNR models therefore omit the antisymmetric contribution. The impact of this approximation on waveform mismatches is discussed in Ref. [23]. We see that the antisymmetric contribution in the coprecessing frame is weak, and in many cases, for example for signals with typical signal-to-noise ratios (SNRs) in the LVK observations to date, we may expect that this approximation is valid. (Reference [24] has verified this for GW190412, which has a SNR of $\sim$19 and no evidence for precession.) However, since we generally require loud signals to measure misaligned spins and precession [25], these are precisely the kinds of signals where the antisymmetric contribution may be important. This point was previously made in Ref. [26], which showed that neglecting the antisymmetric contribution might lead to parameter biases in observations with SNRs as low as 15, depending on the binary's orientation and polarization.

The most striking physical consequence of the multipole asymmetry is out-of-plane recoil of the final black hole [10,27,28]. Reference [29] shows that in the "superkick" configuration (an equal-mass binary with equal spin on each back hole, but with the spins lying in the orbital plane and in opposite directions), the magnitude of the out-of-plane recoil depends sinusoidally on the direction of the spins relative to the separation vector of the two black holes at some reference frequency. The dependence of the phasing of the antisymmetric contribution on the in-plane-spin direction is also discussed in detail in Ref. [30]. Given the dependence of the antisymmetric contribution on the spin direction, and the results in Ref. [26], which looked directly at the distinguishability of waveforms from systems with different in-plane-spin directions, we might expect that the antisymmetric contribution will be important for measuring in-plane spins.

To study this effect, we make use of the surrogate model NRSur7dq4 [31]. This model *does* include the multipole asymmetry, but we also consider a version with the antisymmetric contribution set to zero. In Sec. III we discuss the model in more detail. In Sec. IV we outline our procedure to measure the properties from a series of synthetic signals at high SNR (100), using both the full and symmetric-only versions of the NRSur7dq4 model. The results are presented in Sec. V, where we also consider the LVK observation GW200129_065458 [32] (hereafter referred to as GW200129), which is the first observation for which claims have been made of strong evidence for precession [33] and large recoil [34]. In the next section, however, we will first summarize the features of the multipole asymmetry and the questions we will address in this paper.

II. MULTIPOLE ASYMMETRY AND QUESTIONS FOR STUDY

The multipole asymmetry is discussed in more detail in Ref. [30], but we summarize the main features here, and our expectations for how the asymmetry might impact parameter measurements, to be tested in this work.

The GW multipoles $h_{\ell m}(t)$ may be split into symmetric and antisymmetric contributions. As an example, we write the $(\ell = 2, |m| = 2)$ multipoles as

$$h_{2,2}(t) = A(t)e^{-i\phi_s(t)} + a(t)e^{-i\phi_a(t)}, \quad (3)$$

$$h_{2,-2}(t) = A(t)e^{i\phi_s(t)} - a(t)e^{i\phi_a(t)}, \quad (4)$$

where $A(t)$ and $\phi_s(t)$ are the symmetric amplitude and phase, and $a(t)$ and $\phi_a(t)$ are the antisymmetric amplitude and phase, and $a(t)/A(t) \ll 1$; see Ref. [30] for examples. The amplitude of the antisymmetric contribution $a(t)$ is approximately proportional to the magnitude of the in-plane spin, and $a(t) = 0$ for aligned-spin systems. If we consider single-spin systems in a coprecessing frame, then during the inspiral $\phi_a(t) = \Phi(t) + \alpha(t) + \phi_0$, where $\Phi(t)$ is the binary's orbital phase, $\alpha(t)$ is the precession angle of the black hole's spin and ϕ_0 is an overall constant. These details will be different for the antisymmetric contribution to other multipoles, but a general feature of the antisymmetric contribution to all multipoles is that an overall in-plane spin rotation of $\Delta\alpha$ will introduce a shift of $\Delta\alpha$ into each of the antisymmetric phases. This phase shift manifests itself in out-of-plane recoil. This is discussed in

Ref. [29] for the superkick configurations, where the magnitude of the recoil varies sinusoidally with $\Delta\alpha$.

Given this basic phenomenology of the antisymmetric contribution, we may consider how we expect it to influence measurements of the black-hole masses and spins. We make four points, each of which we will return to in the results of our parameter-estimation study.

(1) Since the antisymmetric part depends on the in-plane spins, we do not expect it (or its absence from a waveform model) to influence parameter measurements unless the signal is strong enough for in-plane spin information to be measurable. This motivates our choice of high SNR signals in our injection study, since in those cases we can be confident that the magnitude and tilt or misalignment angle of each spin with the direction of the orbital angular momentum, $\theta_{\mathrm{LS}_{1,2}}$, should be measurable. Conversely, we expect that the absence of the antisymmetric contribution in a model will lead to biases in the spin measurements, but are less likely to bias parameters that are independent of the in-plane spin components, like the total mass, mass ratio, and aligned-spin combination $\chi_{\mathrm{eff}} = (m_1\boldsymbol{\chi}_1 \cdot \hat{\mathbf{L}} + m_2\boldsymbol{\chi}_2 \cdot \hat{\mathbf{L}})/M$. ($\chi_{\mathrm{eff}}$ affects the inspiral rate [35–37], and therefore the overall binary phasing, at 1.5PN, and so is likely to be measured well regardless of the multipole asymmetry, which cannot enter until at least 2PN [10].) This implies, for example, that the individual aligned-spin components, $\boldsymbol{\chi}_1 \cdot \hat{\mathbf{L}}$ and $\boldsymbol{\chi}_2 \cdot \hat{\mathbf{L}}$, may exhibit significant biases, but the χ_{eff} combination will be fairly well constrained.

(2) As noted above, changes in the initial in-plane-spin direction will introduce an overall phase offset into the antisymmetric contribution, and this affects the out-of-plane recoil. We might expect that the power in the antisymmetric contribution also varies with the in-plane-spin direction, and perhaps there is a correlation: the importance of the antisymmetric contribution in parameter measurements (and the extent of the bias when the antisymmetric contribution is neglected) may be large for cases with large recoil, and small for cases with small recoil. However, the signal's SNR depends on $|h|^2$ as observed at the detector (i.e., from one direction), while the recoil depends on $|\dot{h}|^2$ integrated over the entire sphere. (See Ref. [38] for useful expressions for radiated linear and angular momenta.) There is therefore no reason to expect, for example, that a large recoil in general corresponds to a larger importance of the antisymmetric contribution on the parameter measurements.

(3) The power in the signal is dominated by the symmetric part of the $(\ell = 2, |m| = 2)$ multipole in all of the cases we consider. Even when the signal is nominally edge-on, the majority of the signal power is in the plus polarization, where the total power in the $(\ell = 2, |m| = 2)$ multipoles is comparable in face-on or face-off configurations. Since the overall amplitude of the antisymmetric (2, 2) contribution is a ratio $a(t)/A(t)$ of the symmetric contribution that depends only on the intrinsic parameters of the binary, the fraction of the total power in the antisymmetric contribution will be roughly the same regardless of the orientation. We therefore expect that any biases due to neglecting the antisymmetric contribution will be of similar magnitude regardless of the binary's orientation, for fixed total SNR. This may initially seem counterintuitive from the definition of the asymmetry (we might expect the asymmetry contributions to cancel out for edge-on systems); we explain why this is not the case in Sec. V B.

(4) Since the magnitude of the antisymmetric contribution $a(t)$ depends on the in-plane-spin magnitude, we *do* expect the bias due to neglecting the antisymmetric contribution to be larger for configurations with larger in-plane spins.

These considerations provide us with a series of predictions to test in our injection study: we expect that neglecting the antisymmetric contribution will lead to a bias in the spin measurements, within the broad constraint on the measurement of χ_{eff}, and minimal or no bias in the masses, and that the extent of the bias will be broadly independent of the binary's orientation and recoil, but *will* be roughly proportional to the magnitude of the in-plane spins. We will consider each of these predictions in our results, and find that they hold for most (but not all) of our high-SNR injections. For the GW signal GW200129, however, we find that neglecting the antisymmetric contribution *does* affect the measurement of the mass ratio, although this is a signal where imprints of in-plane spins (i.e., precession) on the signal are only just beyond the threshold of measurability. We also note that our study is limited to single-spin systems; the phenomenology is likely to be more complex in two-spin configurations.

III. WAVEFORM MODEL

Two families of models have been used for most of the LVK measurements of binary properties, PHENOM and SEOBNR [15,18–20,39–42]. As noted above, the versions of these models available through the first three LVK observing runs did not include the multipole asymmetry. A third class of precessing-binary models, NR surrogates, *do* include the multipole asymmetry [31,43,44]. We will use two variants of the NRSur7dq4 model [31] to determine the impact of neglecting the multipole asymmetry in BBH measurements.

The NRSur7dq4 model has been built from numerical relativity simulations with mass ratios $1 \leq q = m_1/m_2 \leq 4$, generic spin directions and spin magnitudes up

to 0.8 and includes all $\ell \leq 4$ spin-weighted spherical-harmonic multipoles. In addition, these NR simulations start at ∼20 orbits or ∼4300M prior to merger. Therefore, the surrogate models are restricted to waveforms of this length and are inadequate whenever longer waveforms are required. Assuming, for example, a waveform with a starting frequency of 20 Hz, the surrogate will only be valid for binaries with total masses $M \gtrsim 65M_\odot$ depending on the mass ratio and the spins of the system [31]. However, within its range of validity NRSur7dq4 is currently the most accurate waveform model available.

To perform a systematics study we isolated the effect of the multipole asymmetry on the parameter estimation results by using two versions of the NRSur7dq4 model, the "full" NRSur7dq4 and the "symmetric" NRSur7dq4. The full NRSur7dq4 is the original NRSur7dq4 waveform model without any alterations. The symmetric NRSur7dq4 is a modified version of this model with the antisymmetric contribution removed, as follows. In the surrogate model, the following contributions are modeled in the coorbital frame,

$$h^{\pm}_{\ell m} = \frac{h^{\mathrm{coorb}}_{\ell m} \pm (-1)^{\ell} h^{\mathrm{coorb}*}_{\ell -m}}{2}. \tag{5}$$

For even ℓ the symmetric contribution is $h^{+}_{\ell m}$ and the antisymmetric contribution is $h^{-}_{\ell m}$, and for odd ℓ it is the reverse. We expect that only the $\ell = 2$ antisymmetric contribution is significant for our results, since the antisymmetric contribution to higher multipoles is in general weaker than the symmetric $\ell = 4$ contributions, and in our analysis we will only use $\ell \leq 3$, as described in Sec. IV. Nonetheless, we consistently remove all antisymmetric contributions in our implementation of the model, i.e., in the symmetric version of the model we set $h^{-}_{\ell m}$ to zero for $\ell = 2$, 4 and set $h^{+}_{\ell m}$ to zero for $\ell = 3$. The symmetric model was constructed from the implementation of NRSur7dq4 in the LALSuite software library [45]. We refer to the symmetric NRSur7dq4 model as NRSur7dq4_sym to simplify notation.

IV. PARAMETER ESTIMATION ANALYSIS

We perform two investigations. In the first we consider synthetic (full) NRSur7dq4 signals with SNR 100, and compare measurements of their parameters using both the full and symmetric versions of NRSur7dq4. In the second, to explore the impact that neglecting multipole asymmetry has on current and near-future observations, we also use the NRSur7dq4 and NRSur7dq4_sym models to analyze the public detector data of the precessing signal GW200129 that have undergone glitch removal, which we refer to as "deglitched" data [32,33]. One aspect of the GW200129 observation not considered in Refs. [33,34] was the impact of the method used to "deglitch" the data. Reference [46] argues that incomplete glitch removal may lead to a spurious precession measurement. However, their analysis is limited by modeling the data as a *nonprecessing* signal plus a glitch; earlier tests on precessing injections [47] may not be sufficient to show that the method can reliably distinguish between precession and glitches, because in each of the test injections the precession contributed insufficient power to be measurable. A more recent analysis, which does not rely on these assumptions [48], suggests that with a more accurate glitch-subtraction procedure, the evidence for precession *increases*. However, for the purposes of the analysis in this paper, where we are concerned with how results vary with respect to different models used to analyze the same set of data, the details of how those data were produced are less relevant.

The analysis is performed using the Markov chain Monte Carlo (MCMC) stochastic sampling technique from the LALInference software library presented in Ref. [49] that was used for the first observing runs, O1-O2 [32,50–53]. For our analysis, we use all three detectors and publicly available power spectral densities that were taken during the O3b observing run. These are the same power spectral densities that were used in the analysis of the GW200129 signal in Refs. [32,33]. The corresponding sensitivity curves of the LIGO Hanford, LIGO Livingston, and Virgo detectors are shown in Fig. 1.

In our parameter estimation analysis, we have chosen to use a flat prior over spin magnitude, the cosine of the tilt angle, and the component masses. The parameter estimation results can be significantly affected by the selected priors of the spin magnitudes and the tilt angles. Since there is no evident justification for employing a prior from the observed population or one motivated by other astrophysical factors, we have selected these particular priors that do not introduce strong assumptions about the underlying

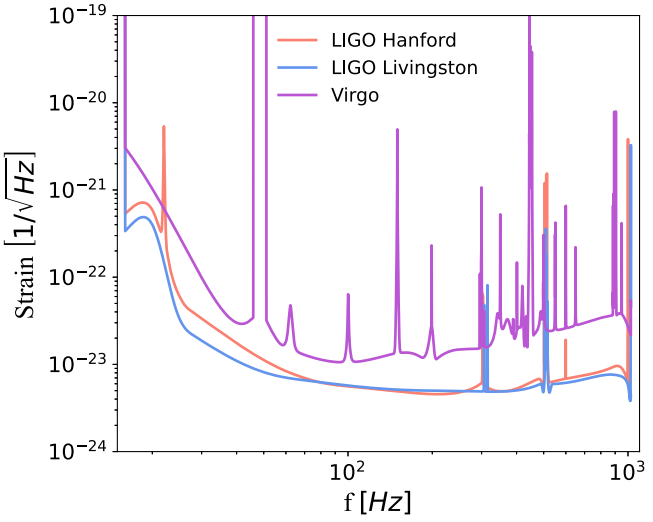

FIG. 1. Amplitude spectral density of the three interferometers' strain sensitivity: LIGO Livingston, LIGO Hanford, Virgo. The square of the amplitude spectral density gives the power spectral density of the detectors.

astrophysical population. These are the default priors that were also used in Refs. [32,33]. Furthermore, the prior parameter space has been adjusted to not exceed significantly the validity range of the surrogate model, setting the total mass to be $M \geq 68M_\odot$, the chirp mass to be within $14.5M_\odot$ and $49M_\odot$, and the mass ratio to be less than 1:4 or 1:6 depending on the configuration. We chose the minimum frequency where the analysis starts to be 20 Hz. The NRSur7dq4 waveforms were generated with starting time that corresponds to 11 Hz for the $(\ell = 2, |m| = 2)$ multipole, to ensure that the highest-frequency multipoles, $(\ell = 3, |m| = 3)$, also start below 20 Hz.

In the case of the NRSur7dq4 injections, the data were all injected with an SNR of 100 and start at 20 Hz using the same basic setup as the O3 catalog [32]. For their sky location, the declination is $\delta = 1.4323$ rads and right ascension $\alpha = 0.2896$ rads, while the polarization is set to $\psi = 1.4$ rads. Each production run produced approximately $\sim 10^5$ samples. Considering that for standard applications of the LALInference sampler 10^4 is a typical amount of samples, we are confident that 10^5 samples is a sufficient number. However, to further ensure the convergence of each run we took into account the behavior of the autocorrelation function and the value of the Gelman-Rubin diagnostic [54].

The NRSur7dq4 data are injected in zero noise, meaning that the detector noise is set to zero while the power spectral densities of the detectors (see Fig. 1) are used to compute the likelihood. In the zero-noise injection, the noise is removed, but the parameter estimation analysis is performed with the relative frequency-dependent sensitivity (noise curve) that corresponds to each detector and for sky location, orientation, and polarization values appropriately also adjusted to the detectors allowing the computation of an SNR. We can interpret the results obtained from this type of injection as an average over many Gaussian noise realizations.

The Gaussian likelihood [55] is given by the noise-weighted inner product [56],

$$\log \mathcal{L} \propto -\langle d(t) - h_M(\theta) | d(t) - h_M(\theta) \rangle, \tag{6}$$

where $h_M(\theta)$ is the waveform model evaluated at parameters θ and $d(t)$ is the data given as the sum of the signal $s(t)$ and $n(t)$ the noise. For a zero-noise injection, since $n(t) = 0$, the data becomes $d(t) = s(t)$ and $\log \mathcal{L} \propto -\langle s(t) - h_M(\theta) | s(t) - h_M(\theta) \rangle$. From the definition of the inner product between two waveforms h_1 and h_2,

$$\langle h_1 | h_2 \rangle = 4\Re \int_0^\infty \frac{h_1(f) h_2^*(f)}{S_n(f)} df, \tag{7}$$

where $S_n(f)$ is the power spectral density, it becomes clear that in the case of the zero-noise injections, the frequency-dependent sensitivity of the detectors is used in the calculation of the likelihood. From the definition of the log likelihood, we note that if the model produces a waveform $h_M(\theta)$ that matches well the signal $s(t)$, the log likelihood $|\log \mathcal{L}|$ has a lower value.

In the case of the GW200129 deglitched data, the parameter estimation analysis is performed using the same settings as those employed in LVK GWTC-3 analysis [32], while also applying the additional settings described in Ref. [33] such as reducing the prior parameter space to fit within the validity range of the NRSur7dq4. For our analysis the waveform is generated at 20 Hz and we have included all the $l \leq 3$ spin-weighted spherical-harmonic multipoles.

A. NRSur7dq4 theoretical waveforms

In the first part of this work, we use the NRSur7dq4 waveform model to investigate how the absence of the multipole asymmetry from the model affects parameter measurement for a number of theoretical signals of strongly precessing binaries with high SNRs. Furthermore, we consider specific configurations that allow us to explore how the biases depend on the recoil velocity of the final black hole, the inclination of the system, the magnitude of the primary black hole's spin, and the mass ratio of the binary, to compare against our phenomenological expectations from Sec. II. In each of these cases the signal is generated from the full NRSur7dq4 waveform model, and the parameter recovery uses the NRSur7dq4 and NRSur7dq4_sym models.

Our fiducial example was a binary with total mass $M = 100M_\odot$, mass ratio $q = 2$, and a dimensionless primary spin magnitude of $a_1/m_1 = 0.7$, with the spin directed entirely in the orbital plane, to maximize precession effects and the antisymmetric contribution. Starting from this basic configuration, we identified initial orientations of the in-plane spin to produce the maximum and minimum possible recoils.

We identified the maximum and minimum recoil by computing the recoil velocities for NRSur7dq4 theoretical waveforms with varying in-plane spin directions of the binaries between 0° and 180°. The in-plane spin direction is denoted by the misalignment angle ϕ_{Sn} between the black holes' separation vector, $\hat{n}$, and the projection of the spin vector $\hat{S}$ on the orbital plane, at the starting frequency. The waveforms were generated in the inertial $\mathbf{L_0}$ frame where $\hat{\mathbf{L}} = \hat{\mathbf{z}}$ at a reference time, satisfying LAL conventions using the LALSimulation function SimInspiralChooseTDModes [45,57]. The recoil velocity was computed from the waveform multipoles [58] in the final $\mathbf{J}$ frame where the z axis is parallel to the total angular momentum, $\mathbf{J}$, of the remnant black hole. Figure 2 shows the measured recoil velocities for different ϕ_{Sn} angles. Based on these results, the lowest recoil velocity is $v_{f_{\min}} = 236$ km/s and the highest is $v_{f_{\max}} = 1461$ km/s. For these two cases the initial in-plane-spin directions ϕ_{Sn} are, respectively, 67° and 138°.

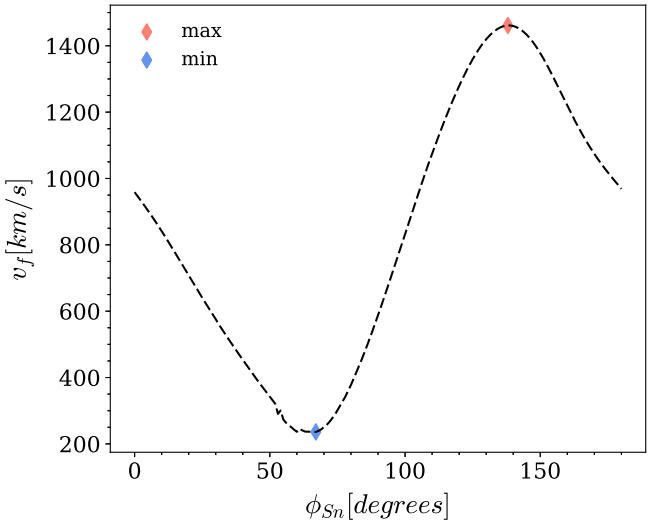

FIG. 2. The minimum (blue) and maximum (red) recoil velocity values and the corresponding in-plane spin direction angles that were selected for this study.

In our signal injections we choose to characterize the binary inclination relative to the direction of maximum asymmetry emission at merger. (This is motivated in Sec. V B.) In general, in precessing systems the binary inclination can be defined in multiple ways: we can consider the orientation of the observer relative to the direction of the total angular momentum, $\mathbf{J}$, which is the closest we have to a fixed direction in precessing binaries. However, if the binary is precessing then by definition $\mathbf{J}$ is *never* the normal to the orbital plane. A common alternative definition of the inclination (adopted in the LAL infrastructure) is the direction of the observer relative to the orbital angular momentum, $\mathbf{L}_0$, at the frequency when the signal enters the detector's sensitivity band. Since $\mathbf{L}$ precesses during inspiral, this definition describes the orientation of the orbital plane to the observer at only one moment; at other points during the inspiral the actual orientation can in principle take on any value. Given these ambiguities, we choose a definition of the inclination relevant to the direction of maximum power in the antisymmetric contribution to the signal.

To do this, we use as a proxy for the merger time t_m the time when the magnitude of the $\ell = 2$ multipoles (added in quadrature) is maximum. We then identify the direction that maximizes the $(\ell = 2, |m| = 2)$ power at t_m (motivated by the definition of the quadrupole-aligned frame [59]); this will also be the direction that maximizes the power in the antisymmetric (2, 2) contribution. We define inclination relative to this direction, i.e., $\iota = 0°$ corresponds to the observer being face-on to the direction of maximum emission at merger. In practice, to impose this in our injections using the LAL infrastructure, we first rotated our signal multipoles so that the maximum emission at t_m was along the z axis, and then prevented LAL from performing a frame rotation by artificially setting $\hat{\mathbf{L}}$ to be along the z axis in the waveform metadata.

The two NRSur7dq4 waveforms (corresponding to maximum and minimum recoil) were injected with different inclinations, varying from 0° to 90° in steps of 30°. This allowed us to investigate how the inclination of the detected system affects the biases that the asymmetry's absence may introduce in the parameter estimation results.

In addition, to test how the NRSur7dq4_sym model behaves for different mass ratios and spin magnitudes, we performed two additional injections. The selected configurations for that purpose are a binary black hole configuration with mass ratio $q = 2$ and a smaller in-plane spin of magnitude $a_1/m_1 = 0.4$, and a binary with a higher mass ratio $q = 4$ and slightly higher in-plane spin of magnitude $a_1/m_1 = 0.8$. In these last two cases, the in-plane spin direction is $\phi_{Sn} = 0°$ and the total mass of this binary is $M = 100M_\odot$. The selected inclination is $\iota = 60°$ and they are both injected at SNR 100. For these additional injections we use the standard LAL definition of inclination.

To summarize, we performed 20 parameter-estimation analyses of ten configurations using the NRSur7dq4 and NRSur7dq4_sym models: the maximum- and minimum-recoil versions of the fiducial configuration, at orientations $\iota = 0°, 30°, 60°, 90°$ and two additional single-spin configurations $(q = 2, a_1/m_1 = 0.4, \theta_{\mathrm{LS}_1} = 90°)$ and $(q = 4, a_1/m_1 = 0.8, \theta_{\mathrm{LS}_1} = 90°)$ at orientation $\iota = 60°$. We will show results from a representative subset of these analyses in Sec. V.

B. GW200129 gravitational wave signal

In the second part of this work, we consider the GW200129 gravitational wave signal that was first reported in Ref. [32]. Reference [33] presented strong evidence that GW200129 was the first GW observation of a precessing binary, with masses $m_1 = 39M_\odot$ and $m_2 = 22M_\odot$, and the primary black hole rapidly spinning with $a_1/m_1 = 0.9$, and the spin lying almost entirely in the orbital plane. The measured parameters of the signal calculated with the NRSur7dq4 are displayed in Table 1 of Ref. [33]. The total network SNR of GW200129 is 26.5 and the SNRs in each detector were measured to be 14.6 in Hanford, 21.2 in Livingston, and 6.3 in Virgo. Reference [34] also showed that the GW200129 has a large recoil velocity of $v_f = 1542$ km/s, which suggests that the antisymmetric contribution to the signal was measurable and could significantly influence the parameter estimates.

We test the importance of the antisymmetric contribution by also analyzing GW200129 with NRSur7dq4_sym. As noted in Sec. IV, besides the change in the model used in the analysis, all other settings are the same as in the analysis reported in Ref. [33].

V. RESULTS

We present our results as follows. We first consider the importance of the multipole asymmetry on measurements of our fiducial high-SNR configuration, in Sec. V A; this allows us to examine the first expectation from Sec. II. We then consider the remaining expectations (2–4) in Sec. V B by considering variations in recoil, orientation, and mass-ratio and spin magnitude. We then look at the importance of the multipole asymmetry on GW200129 in Sec. V C.

A. The impact of the antisymmetric contribution

In this section we will show a subset of results that illustrate the impact of the mode asymmetry that we observe from our parameter-estimation analyses. Our fiducial configuration is $(q = 2, a_1/m_1 = 0.7, a_2/m_2 = 0, \theta_{\mathrm{LS}_1} = 90°)$, and in Fig. 3 we show results for the initial in-plane spin orientation that leads to minimal recoil ($\phi_{Sn} = 67°$, top row) and maximum recoil ($\phi_{Sn} = 138°$, middle row), both at inclination $\iota = 30°$ with respect to the direction of maximum emission at merger. The bottom row shows the minimum recoil configuration viewed at $\iota = 90°$.

Our first expectation from Sec. II was that measurements of the masses and χ_{eff} would not be biased by neglecting the multipole asymmetry. Figure 3 shows the measurements for M, q, and χ_{eff} for three configurations, and we see that to some extent our expectation holds, in that the measured values are only slightly affected by the symmetric

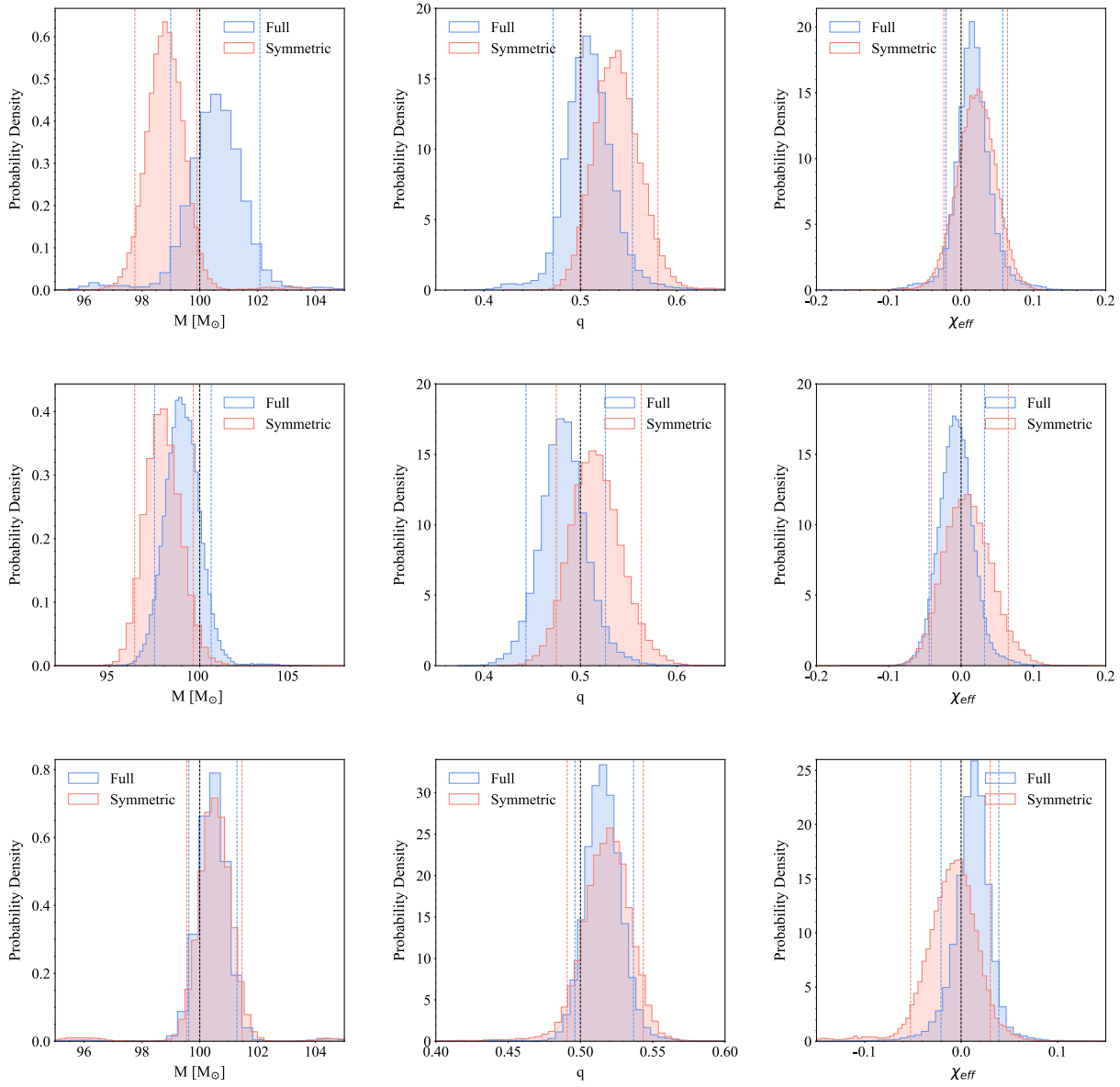

FIG. 3. Measurements of M, q, and χ_{eff} for the $(q = 2,\ a_1/m_1 = 0.7,\ a_2/m_2 = 0,\ \theta_{\mathrm{LS}_1} = 90°)$ configurations with (top) $\iota = 30°$, minimum recoil, (middle) $\iota = 30°$, maximum recoil, and (bottom) $\iota = 90°$, minimum recoil, as they were measured by the NRSur7dq4 (blue) and NRSur7dq4_sym (red) models.

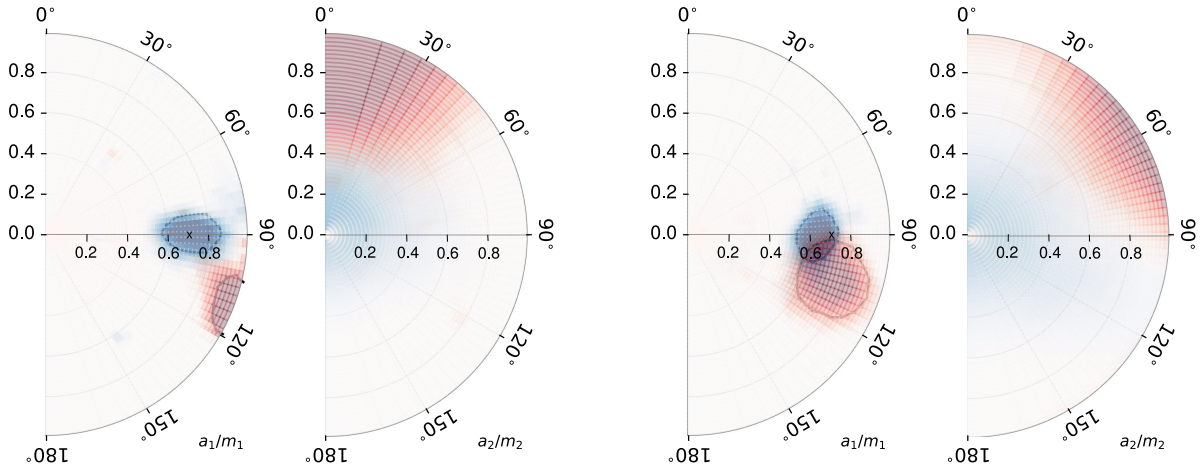

FIG. 4. Magnitude and direction of each spin, a_1/m_1 and a_2/m_2, for ($q = 2$, $a_1/m_1 = 0.7$, $a_2/m_2 = 0$, $\theta_{\mathrm{LS}_1} = 90°$) configurations at inclination $\iota = 30°$ as they were measured by the NRSur7dq4 (blue) and NRSur7dq4_sym (red) models. Left: the configuration with initial in-plane-spin direction chosen to yield minimum recoil. Right: the configuration with maximum recoil.

approximation in NRSur7dq4_sym. Nonetheless, we do see *some* bias; in the top and middle panels the true value of the mass and/or mass ratio lies outside the 90% confidence interval. In several measurements shown here (and similarly in the other configurations we studied), there is a less clear sign of bias.

We now look at the individual spin magnitudes and tilt angles. These are shown for the minimum-recoil configuration in the left panel of Fig. 4.

In each disk plot, the spin magnitude is between 0 and 1 while the tilt angle ranges between 0° and 180°, where 0° corresponds to an aligned-spin system where the spins are in the same direction as the orbital angular momentum. The shading indicates the parameters' measured values and the different colors correspond to the results from the recovery with the two versions of the surrogate model.

We see that the recovered spin magnitude and the tilt angle of the primary black hole with NRSur7dq4_sym have a higher value, indicating that the spin vector lies outside the plane of the binary. Furthermore, the recovered spin magnitude reaches the Kerr limit, $a_1/m_1 = 1$. In contrast, the measured parameters with the NRSur7dq4 agree well with the true values. A similar behavior can be observed for a_2/m_2. The true spin of the secondary black hole is zero, as recovered well with the NRSur7dq4 model. However, the NRSur7dq4_sym model measures a high spin value for the same black hole and a low tilt angle, i.e., the spin appears nearly aligned with the orbital angular momentum.

Despite the significant biases in the spin measurements with the NRSur7dq4_sym model, we do see, as expected, that the combination χ_{eff} is measured correctly; the biases counteract so that χ_{eff} has the correct value. We saw similar results in all of the fiducial-configuration binaries: the NRSur7dq4_sym recovery for a_1/m_1 and a_2/m_2 varied in magnitude and direction, but always such that χ_{eff} was roughly correct. We might expect, however, that in larger-mass-ratio binaries with sufficiently high spin on the primary, that the spin measurements will rail against the Kerr limit, and it will not be possible for the biases to fully counteract each other to give a correct value of χ_{eff}. We will see examples of this in the next section.

B. Dependence on recoil, inclination, spin magnitude, and mass ratio

We now consider how the impact of the multipole asymmetry varies with the recoil (or, equivalently, changes in the initial in-plane-spin direction), the binary's inclination to the detector, the spin magnitude, and the mass ratio.

As noted in Sec. II, although changes in the initial in-plane-spin direction will change the out-of-plane recoil of the final black hole, we do not necessarily expect this to qualitatively change the bias due to neglecting the multipole asymmetry. This is borne out in the right-hand panel of Fig. 4, which shows the recovery of the spins for the same system, but now with $\phi_{Sn} = 138°$ and maximum recoil. We see that the details of the spin measurements from the NRSur7dq4_sym model differ—the primary spin magnitude a_1/m_1 is closer to the correct value, but the secondary spin magnitude a_2/m_2 shows a stronger preference for extreme spins—but qualitatively the results are similar.

We next consider how the impact of the asymmetry changes with inclination. We noted in Sec. II that we do not expect the effects to change significantly with inclination. Let us explain this further. Naively, the impact of the asymmetry *does* have a clear dependence on inclination. If we write the (2, 2) multipoles as $h_{2,\pm 2} = h_s \pm h_a$, where h_s and h_a are the symmetric and antisymmetric contributions [as in Eqs. (3) and (4)], then the strain as a function of the inclination with respect to the normal to the orbital plane θ and azimuthal angle φ is given by

$$h(\theta,\varphi) = h_{2,2}{}^{-2}Y_{2,2}(\theta,\varphi) + h_{2,-2}{}^{-2}Y_{2,-2}(\theta,\varphi). \quad (8)$$

The spherical harmonics depend on θ as $(1 \pm \cos\theta)^2$, and so the relative strength R_{as} of the antisymmetric and symmetric contributions, compared to their relative strength at $\theta = 0$, is

$$R_{as} = \frac{4\cos\theta}{3 + \cos(2\theta)}. \quad (9)$$

From this we see that edge-on to the binary, $\theta = \pi/2$, the antisymmetric contributions will cancel out. However, in a precessing system we can never be edge-on to the binary at all times.

In our fiducial configuration $(q = 2, a_1/m_1 = 0.7, a_2/m_2 = 0, \theta_{\mathrm{LS}_1} = 90°)$, the maximum opening angle between the orbital angular momentum and the total angular momentum is $\beta_{\max} \approx 0.35$. (See Fig. 8 in Ref. [17].) If we were to define inclination with respect to $\mathbf{J}$, then a nominal inclination of $\pi/2$ would correspond to an inclination with respect to the orbital plane of $\pi/2 - 0.35$, and $R_{as} = 0.61$. If we were to define the inclination with respect to the orbital angular momentum when the signal enters the detector's sensitivity band (as is the standard LAL convention), then depending on where this point lies in the precession cycle, the inclination relative to the normal to the orbital plane at merger could be as large as $2\beta_{\max} \approx 0.7$, with $R_{as} = 0.91$. This illustrates the nontrivial importance of how we define inclination.

This motivated the inclination we have used for these analyses, where $\iota = 0$ corresponds to the direction of maximum emission at merger. With this definition, we expect that $\iota = \pi/2$ will correspond to the binary being edge-on to the detector at merger (i.e., the peak in the signal amplitude), and therefore zero contribution from the asymmetry at merger. At all other times the signal is weaker and the opening angle β is smaller, and so we may hope to minimize the impact of the asymmetry on parameter measurements.

The lower panel of Fig. 3 shows M, q, and χ_{eff} for an inclination of $\iota = 90°$. In this case we do not see any clear sign of bias, which suggests that we may have removed the impact of the antisymmetric contribution. (Similarly, we see slightly larger biases in $\iota = 0$ cases.) However, Fig. 5 shows the spin measurements for the $\iota = 90°$ signal, and we see that some bias remains. It appears to be smaller than in the $\iota = 30°$ signals, but has not been significantly reduced. For any given configuration there will be some inclination that minimizes the impact of the asymmetry, but given that the inclination oscillates due to precession, and R_{as} is approximately one up to $\theta \approx 1$ rad, we conclude that the impact of the asymmetry does not in general depend significantly on the binary orientation. We did not attempt to identify a specific relationship between the details of the biases and the choices of inclination and total recoil, but this would be interesting to study further in the future.

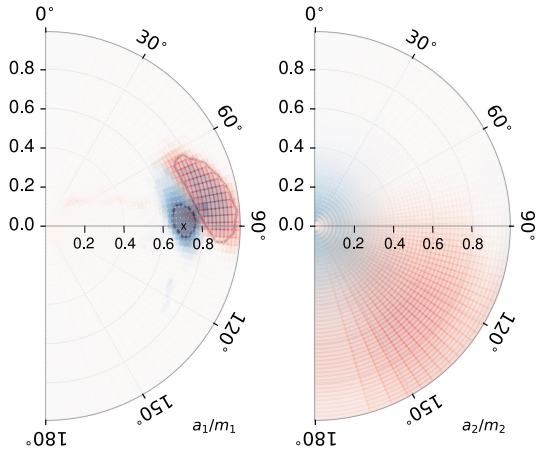

FIG. 5. Spin magnitude and direction of (left) a_1/m_1 and (right) a_2/m_2 of the minimum recoil ($q = 2$, $a_1/m_1 = 0.7$, $a_2/m_2 = 0$, $\theta_{\mathrm{LS}_1} = 90°$) configuration's black holes with inclination 90° as they were measured by the NRSur7dq4 (blue) and NRSur7dq4_sym (red) models.

Finally, we consider changes in the spin magnitude and mass ratio: a lower-spin system $(q = 2, a_1/m_1 = 0.4, a_2/m_2 = 0, \theta_{\mathrm{LS}_1} = 90°)$, and a system with larger mass ratio and larger spin $(q = 4, a_1/m_1 = 0.8, a_2/m_2 = 0, \theta_{\mathrm{LS}_1} = 90°)$.

We see in the top row of Fig. 6 that in the lower-spin case the posteriors for M, q, and χ_{eff} are wider in the analysis with the NRSur7dq4_sym model, but we still do not see any significant bias, except for a shoulder in the M posterior in one case. This is consistent with our expectation that a lower spin magnitude will also lower the impact of the multipole asymmetry. For the high-mass-ratio case (bottom row), there is more sign of biases. The posteriors from the NRSur7dq4_sym recovery are much broader that for the NRSur7dq4, especially for the total mass, where the width of the 90% confidence region has almost doubled. We also see that there is now a clear bias in χ_{eff} when recovering with the NRSur7dq4_sym model.

Figure 7 shows the spin magnitudes and tilt angles for the lower-spin and higher-mass-ratio cases. As we expect, the bias is reduced when the spin magnitude is reduced, and in this case there is no clear bias in the measurement of the primary spin, and the secondary spin, although it appears biased in the disk plots, the real difference between the NRSur7dq4 and NRSur7dq4_sym models analyses is that with NRSur7dq4 the second spin magnitude is constrained by less than 0.45, while with the NRSur7dq4_sym the second spin is not constrained; the 90% confidence interval covers 90% of the parameter range.

The high-mass-ratio case is more interesting. It now appears that the primary spin can be measured accurately with both models, suggesting that the spin imprint on the

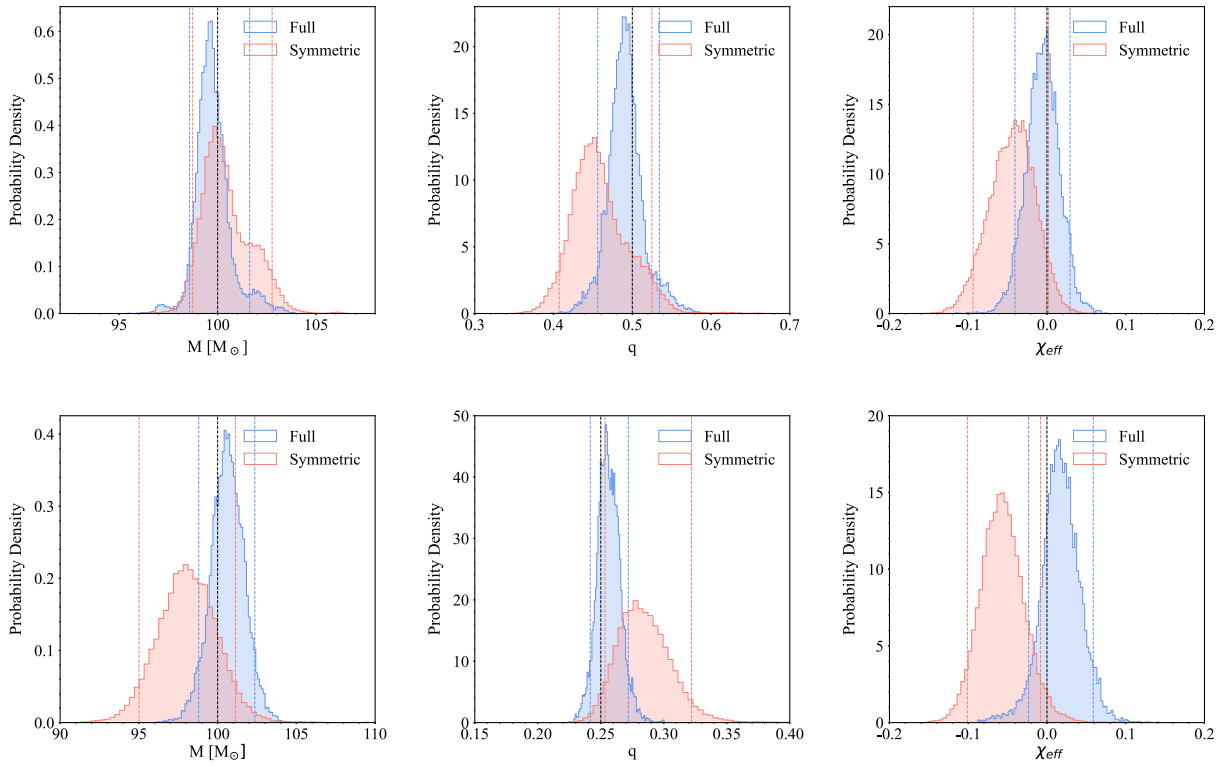

FIG. 6. Measurements of M, q, and $\chi_{\rm eff}$ for the (top) ($q=2$, $a_1/m_1=0.4$, $a_2/m_2=0$, $\theta_{\rm LS_1}=90°$) and (bottom) ($q=4$, $a_1/m_1=0.8$, $a_2/m_2=0$, $\theta_{\rm LS_1}=90°$) configurations as they were measured by the NRSur7dq4 (blue) and NRSur7dq4_sym (red) models.

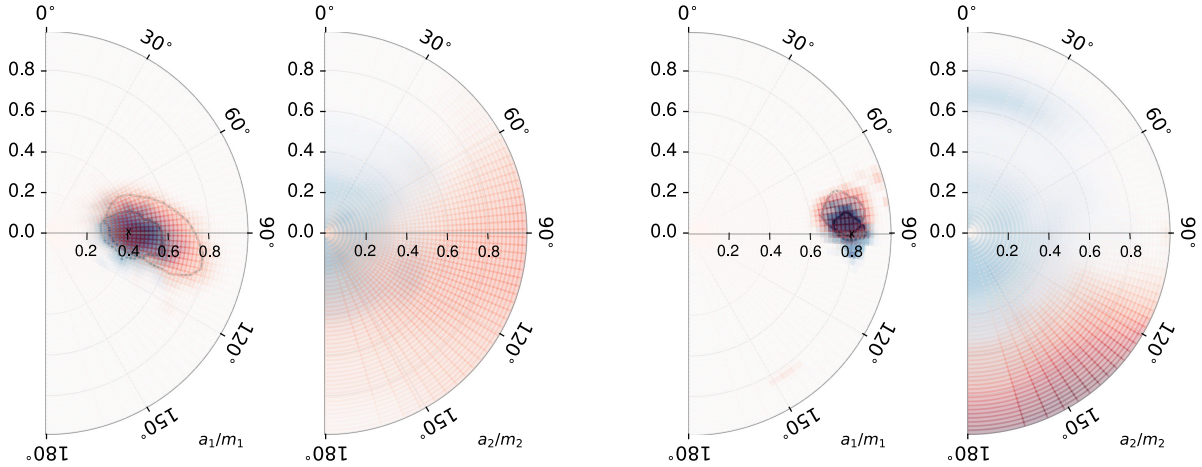

FIG. 7. Spin magnitude and direction of a_1/m_1 and a_2/m_2 of the (left) ($q=2$, $a_1/m_1=0.4$, $a_2/m_2=0$, $\theta_{\rm LS_1}=90°$) and (right) ($q=4$, $a_1/m_1=0.8$, $a_2/m_2=0$, $\theta_{\rm LS_1}=90°$) configurations, both with inclination $\iota=60°$ as they were measured by the NRSur7dq4 (blue) and NRSur7dq4_sym (red) models.

symmetric contribution to the signal is strong enough to constrain the value. This is not the case for the secondary spin, and without the antisymmetric contribution to the model the secondary spin is biased. The bias in this sector of the model also appears to be so strong that it is no longer counteracted by the inspiral phasing that plays the dominant role in determining $\chi_{\rm eff}$, and so this is now also biased. We expect that this is a general trend: at higher mass ratios ($q \gtrsim 4$) the measurement of the primary spin is more reliable than quantities that include both spins. Since there is a partial degeneracy between the mass ratio and $\chi_{\rm eff}$ [35,36,60], the bias in $\chi_{\rm eff}$ also leads to a bias in the mass ratio.

C. GW200129 signal

We now consider the gravitational-wave signal GW200129. The measured parameters presented in Refs. [32,33] indicate that this system is similar to some of the injected NRSur7dq4 waveforms that were discussed in the previous section. However, interestingly in this case the SNR is only 26.5 making this signal significantly weaker compared to the theoretical signals of the previous section. As a result, we expect the effects of the absence of the asymmetry to be more subtle.

As previously, we analyze the signal with the NRSur7dq4 and NRSur7dq4_sym models. As shown in Table I, the total mass, M, is recovered consistently with the two versions of the NRSur7dq4. However, the measurements of the mass ratio, q, and the individual masses, m_1 and m_2, differ between the two models. The results presented in Fig. 8 show that the full NRSur7dq4 model measures that this is an unequal-mass system while the measurement of the mass ratio with the NRSur7dq4_sym model is not well constrained. Furthermore, the primary spin measurements presented in Fig. 8 show that the recovery with both versions of the surrogate lead to similar results for the tilt angle. However, in the case of the primary spin magnitude, this is poorly constrained with the NRSur7dq4_sym, while it is clearly identified as a high spin by NRSur7dq4.

From these results it becomes evident that, even at relatively low SNR, including the asymmetry in the model was essential in identifying this system as an unequal-mass binary with large in-plane spin. We note that in the LVK analyses of this signal, which used the IMRPhenomXPHM and SEOBNRv4PHM models, the IMRPhenomXPHM results showed some support for unequal masses and high spin. However, since this model does not include the multipole asymmetry, it is possible that the apparent measurement of a high primary spin was due to uncertainties in the waveform

TABLE I. The recovered parameters for the deglitched GW200129 data with their 90% credible intervals. The results were recovered using the NRSur7dq4 and NRSur7dq4_sym models. (The effective precession spin, χ_p, is defined in Refs. [39,61]).

	Full	Symmetric
Primary mass, $m_1(M_\odot)$	$47.62^{+6.17}_{-8.88}$	$42.48^{+11.0}_{-4.94}$
Secondary mass, $m_2(M_\odot)$	$27.0^{+8.83}_{-4.96}$	$32.54^{+4.64}_{-9.73}$
Mass ratio, $q = m_2/m_1$	$0.57^{+0.36}_{-0.15}$	$0.77^{+0.21}_{-0.34}$
Total mass, $M = m_1 + m_2(M_\odot)$	$74.83^{+3.06}_{-3.07}$	$75.28^{+3.06}_{-3.27}$
Primary spin, a_1/m_1	$0.88^{+0.11}_{-0.45}$	$0.68^{+0.31}_{-0.58}$
Primary spin tilt angle, $\theta_{\mathrm{LS}_1}(rad)$	$1.41^{+0.37}_{-0.46}$	$1.32^{+0.74}_{-0.76}$
χ_{eff}	$0.06^{+0.12}_{-0.12}$	$0.12^{+0.09}_{-0.14}$
χ_p	$0.85^{+0.13}_{-0.37}$	$0.66^{+0.31}_{-0.45}$

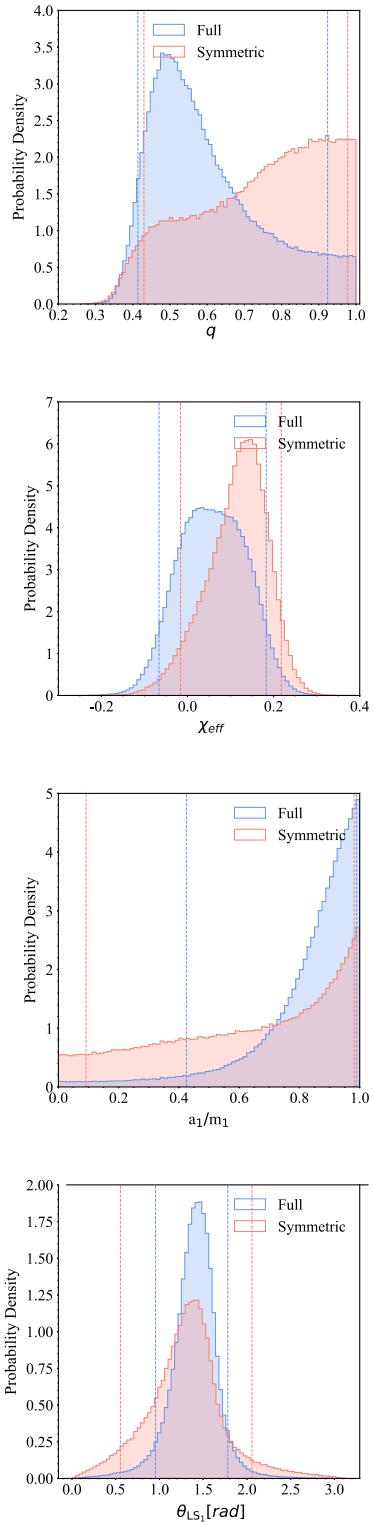

FIG. 8. One-dimensional posterior distributions for the mass ratio, χ_{eff}, primary spin magnitude, and tilt angle, for the NRSur7dq4 (blue) and NRSur7dq4_sym (red) recovery of GW200129.

model (as suggested in Refs. [33,62]), and its partial agreement with the results from the more accurate and complete NRSur7dq4 model may have been coincidental. To fully clarify these questions would require a more detailed study of the uncertainties of all three models in this region of parameter space, but since the PHENOM and SEOBNR models have now both been superseded by upgraded versions [63,64], these points may be moot. The broader and more important conclusion that we can draw from these results is that further improvement in symmetric models alone will not be sufficient to accurately measure the parameters of precessing systems, even at moderate SNRs; the inclusion of the multipole asymmetry is required in all waveform models.

VI. CONCLUSION

We have studied the impact of neglecting the multipole asymmetry in waveform modeling on the measurement of binary source parameters. We focused on loud signals (with SNR 100) to assess the impact of the multipole asymmetry in systems where the individual spins should be measurable. We find that neglecting the multipole asymmetry introduces systematic errors into the measurement of the magnitude and direction of each spin. The parameters that are measured in the absence of precession (M, q, $\chi_{\rm eff}$) are only weakly affected by neglecting the asymmetry, at least for systems with comparable masses or small spins.

Furthermore, we investigate how the biases depend on the inclination of the binary, the primary spin magnitude, and the mass ratio of the system. We also test their dependence on the recoil velocity of the final black hole by injecting NRSur7dq4 waveforms with different in-plane spin directions that correspond to the maximum and minimum recoil. Our results show no evidence of strong dependence between the biases and the recoil velocity or the inclination of the system. We find that for the inclinations we consider, $\iota \in [0°, 30°, 60°, 90°]$, there is no strong impact on the biases even if the system is oriented from face-on to edge-on. Similarly, in the case of the maximum and minimum recoil value, the magnitude of the biases remains largely unaffected by these extremes in the recoil values. Across all of these cases, the bias in the spin magnitudes and directions will vary as these parameters are changed, but the biases do not become particularly larger or smaller. We leave a detailed understanding of the direction and magnitude of the biases as a function of inclination and spin direction to future work.

In contrast, the biases introduced by the NRSur7dq4_sym model do depend on the primary spin magnitude and the mass ratio of the system. We investigate these effects for configurations with two different primary spin values $a_1/m_1 = 0.4$, 0.7. Since the effects of the multipole asymmetry are weaker for lower spins, the biases are more subtle in the analysis of the biniary with spin $a_1/m_1 = 0.4$. To test the dependency on the mass ratio, we considered binaries with mass ratios $q = 2, 4$. In addition, we consider a higher-mass-ratio, high-spin configuration, and here the primary spin is better constrained by the symmetric model, but the secondary spin rails against extremal values, and this in turn does lead to a bias in $\chi_{\rm eff}$.

We have also considered the GW200129 signal, which is the only GW observation so far to show strong evidence for precession [33]. We find that without the multipole asymmetry it is not possible to reliably identify the high primary spin (the lower bound of the 90% credible interval drops from 0.43 to 0.1), and the mass ratio is less well constrained; see Fig. 8 and Table I. This illustrates the importance of the multipole asymmetry in measurements of precessing binaries, even at relatively low SNRs. This example also illustrates the confusing systematic errors that can be introduced by model uncertainty: in the LVK analysis the IMRPhenomXPHM model may by spuriously identifying a high primary spin due to inaccuracies in the symmetric contribution (since we find that an accurate symmetric model does not identify a high spin).

These results have important consequences for future observations of binary black holes. As detector sensitivities improve, we will observe more systems at SNRs where it is in principle possible to measure the full spin information (both "aligned" and "in-plane" components). Employing symmetric waveforms for the analysis of these signals will lead to incorrect measurements, making it difficult to confidently identify precessing systems, and to measure the spin magnitudes and orientations, and the recoil. This will likely also impact population studies and efforts to better understand binary formation mechanisms.

The current study used the NRSur7dq4 model, which does include multipole asymmetry. However, this model cannot be used for systems with large mass ratios, or masses below $65M_\odot$. Our results show that it is essential to include the multipole asymmetry in other waveform models. An approach to do this for frequency-domain models was recently presented in Ref. [30], and this or other methods need to be developed for any waveform model intended for use on signals beyond moderate SNRs, where in-plane spin information may be measurable.

ACKNOWLEDGMENTS

We thank Charlie Hoy for discussions and assistance with parameter estimation analyses, and Lionel London for sharing his numerical-relativity data processing tools. We also thank Steve Fairhurst, Vivien Raymond, Frank Ohme, Patricia Schmidt, and Geraint Pratten for discussions. The authors were supported in part by Science and Technology Facilities Council (STFC) Grant No. ST/V00154X/1 and European Research Council (ERC) Consolidator Grant No. 647839. P. K. was also supported by the GW consolidated grant: STFC Grant No. ST/V005677/1. J. T. acknowledges support from the NASA LISA Preparatory Science Grant No. 20-LPS20-0005. This research was undertaken using the supercomputing

facilities at Cardiff University operated by Advanced Research Computing at Cardiff (ARCCA) on behalf of the Cardiff Supercomputing Facility and the HPC Wales and Supercomputing Wales (SCW) projects. We acknowledge the support of the latter, which is part-funded by the European Regional Development Fund (ERDF) via the Welsh Government. Plots were prepared with Matplotlib [65] and PESummary [66]. Parameter estimation was performed with the LALInference software library [49]. NumPy [67] and Scipy [68] were also used during our analysis.

[1] R. Abbott *et al.* (LIGO Scientific and Virgo Collaborations), Astrophys. J. Lett. **913**, L7 (2021).
[2] R. Abbott *et al.* (KAGRA, Virgo, and LIGO Scientific Collaborations), Phys. Rev. X **13**, 011048 (2023).
[3] B. P. Abbott *et al.* (LIGO Scientific and Virgo Collaborations), Astrophys. J. Lett. **818**, L22 (2016).
[4] B. P. Abbott *et al.* (LIGO Scientific and Virgo Collaborations), Astrophys. J. Lett. **882**, L24 (2019).
[5] J. Aasi, B. P. Abbott, R. Abbott, T. Abbott, M. R. Abernathy, K. Ackley, C. Adams, T. Adams, P. Addesso *et al.* (LIGO Scientific Collaboration), Classical Quantum Gravity **32**, 074001 (2015).
[6] F. a. Acernese, M. Agathos, K. Agatsuma, D. Aisa, N. Allemandou, A. Allocca, J. Amarni, P. Astone, G. Balestri, G. Ballardin *et al.*, Classical Quantum Gravity **32**, 024001 (2014).
[7] T. Akutsu, M. Ando *et al.* (KAGRA Collaboration), Nat. Astron. **3**, 35 (2019).
[8] P. Ajith *et al.*, Phys. Rev. Lett. **106**, 241101 (2011).
[9] T. A. Apostolatos, C. Cutler, G. J. Sussman, and K. S. Thorne, Phys. Rev. D **49**, 6274 (1994).
[10] L. E. Kidder, Phys. Rev. D **52**, 821 (1995).
[11] P. Schmidt, M. Hannam, and S. Husa, Phys. Rev. D **86**, 104063 (2012).
[12] M. Hannam, P. Schmidt, A. Bohé, L. Haegel, S. Husa, F. Ohme, G. Pratten, and M. Pürrer, Phys. Rev. Lett. **113**, 151101 (2014).
[13] S. Khan, K. Chatziioannou, M. Hannam, and F. Ohme, Phys. Rev. D **100**, 024059 (2019).
[14] S. Khan, F. Ohme, K. Chatziioannou, and M. Hannam, Phys. Rev. D **101**, 024056 (2020).
[15] G. Pratten *et al.*, Phys. Rev. D **103**, 104056 (2021).
[16] H. Estellés, M. Colleoni, C. García-Quirós, S. Husa, D. Keitel, M. Mateu-Lucena, M. d. L. Planas, and A. Ramos-Buades, Phys. Rev. D **105**, 084040 (2022).
[17] E. Hamilton, L. London, J. E. Thompson, E. Fauchon-Jones, M. Hannam, C. Kalaghatgi, S. Khan, F. Pannarale, and A. Vano-Vinuales, Phys. Rev. D **104**, 124027 (2021).
[18] Y. Pan, A. Buonanno, A. Taracchini, L. E. Kidder, A. H. Mroué, H. P. Pfeiffer, M. A. Scheel, and B. Szilágyi, Phys. Rev. D **89**, 084006 (2014).
[19] A. Taracchini, A. Buonanno, Y. Pan, T. Hinderer, M. Boyle, D. A. Hemberger, L. E. Kidder, G. Lovelace, A. H. Mroué, H. P. Pfeiffer, M. A. Scheel, B. Szilágyi, N. W. Taylor, and A. Zenginoglu, Phys. Rev. D **89**, 061502 (2014).
[20] S. Ossokine, A. Buonanno, S. Marsat, R. Cotesta, S. Babak, T. Dietrich, R. Haas, I. Hinder, H. P. Pfeiffer, M. Pürrer, C. J. Woodford, M. Boyle, L. E. Kidder, M. A. Scheel, and B. Szilágyi, Phys. Rev. D **102**, 044055 (2020).
[21] A. Ramos-Buades, A. Buonanno, H. Estellés, M. Khalil, D. P. Mihaylov, S. Ossokine, L. Pompili, and M. Shiferaw, arXiv:2303.18046.
[22] M. Boyle, L. E. Kidder, S. Ossokine, and H. P. Pfeiffer, arXiv:1409.4431.
[23] A. Ramos-Buades, P. Schmidt, G. Pratten, and S. Husa, Phys. Rev. D **101**, 103014 (2020).
[24] T. Islam, S. E. Field, C.-J. Haster, and R. Smith, Phys. Rev. D **103**, 104027 (2021).
[25] R. Green, C. Hoy, S. Fairhurst, M. Hannam, F. Pannarale, and C. Thomas, Phys. Rev. D **103**, 124023 (2021).
[26] C. Kalaghatgi and M. Hannam, Phys. Rev. D **103**, 024024 (2021).
[27] J. A. González, M. Hannam, U. Sperhake, B. Brügmann, and S. Husa, Phys. Rev. Lett. **98**, 231101 (2007).
[28] M. Campanelli, C. O. Lousto, Y. Zlochower, and D. Merritt, Astrophys. J. Lett. **659**, L5 (2007).
[29] B. Bruegmann, J. A. Gonzalez, M. Hannam, S. Husa, and U. Sperhake, Phys. Rev. D **77**, 124047 (2008).
[30] S. Ghosh, P. Kolitsidou, and M. Hannam, Phys. Rev. D **109**, 024061 (2024).
[31] V. Varma, S. E. Field, M. A. Scheel, J. Blackman, D. Gerosa, L. C. Stein, L. E. Kidder, and H. P. Pfeiffer, Phys. Rev. Res. **1**, 033015 (2019).
[32] R. Abbott *et al.* (LIGO Scientific, Virgo, and KAGRA Collaborations), Phys. Rev. X **13**, 041039 (2023).
[33] M. Hannam *et al.*, Nature (London) **610**, 652 (2022).
[34] V. Varma, S. Biscoveanu, T. Islam, F. H. Shaik, C.-J. Haster, M. Isi, W. M. Farr, S. E. Field, and S. Vitale, Phys. Rev. Lett. **128**, 191102 (2022).
[35] C. Cutler and E. E. Flanagan, Phys. Rev. D **49**, 2658 (1994).
[36] E. Poisson and C. M. Will, Phys. Rev. D **52**, 848 (1995).
[37] P. Ajith, Phys. Rev. D **84**, 084037 (2011).
[38] M. Ruiz, M. Alcubierre, D. Núñez, and R. Takahashi, Gen. Relativ. Gravit. **40**, 1705 (2008).
[39] M. Hannam, P. Schmidt, A. Bohé, L. Haegel, S. Husa, F. Ohme, G. Pratten, and M. Pürrer, Phys. Rev. Lett. **113**, 151101 (2014).
[40] S. Khan, F. Ohme, K. Chatziioannou, and M. Hannam, Phys. Rev. D **101**, 024056 (2020).
[41] M. Pürrer, Phys. Rev. D **93**, 064041 (2016).
[42] A. Bohé *et al.*, Phys. Rev. D **95**, 044028 (2017).
[43] J. Blackman, S. E. Field, M. A. Scheel, C. R. Galley, D. A. Hemberger, P. Schmidt, and R. Smith, Phys. Rev. D **95**, 104023 (2017).

[44] J. Blackman, S. E. Field, M. A. Scheel, C. R. Galley, C. D. Ott, M. Boyle, L. E. Kidder, H. P. Pfeiffer, and B. Szilágyi, Phys. Rev. D **96**, 024058 (2017).
[45] LIGO Scientific Collaboration, LIGO Algorithm Library, 10.7935/GT1W-FZ16 (2018).
[46] E. Payne, S. Hourihane, J. Golomb, R. Udall, R. Udall, D. Davis, and K. Chatziioannou, Phys. Rev. D **106**, 104017 (2022).
[47] S. Hourihane, K. Chatziioannou, M. Wijngaarden, D. Davis, T. Littenberg, and N. Cornish, Phys. Rev. D **106**, 042006 (2022).
[48] R. Macas, A. Lundgren, and G. Ashton, Phys. Rev. D **109**, 062006 (2024).
[49] J. Veitch, V. Raymond, B. Farr, W. Farr, P. Graff, S. Vitale, B. Aylott, K. Blackburn, N. Christensen, M. Coughlin *et al.*, Phys. Rev. D **91**, 042003 (2015).
[50] B. P. Abbott *et al.* (LIGO Scientific and Virgo Collaborations), Phys. Rev. Lett. **116**, 061102 (2016).
[51] B. P. Abbott *et al.* (LIGO Scientific and Virgo Collaborations), Phys. Rev. X **9**, 031040 (2019).
[52] R. Abbott *et al.* (LIGO Scientific and Virgo Collaborations), Phys. Rev. X **11**, 021053 (2021).
[53] B. P. Abbott *et al.* (LIGO Scientific and Virgo Collaborations), Phys. Rev. D **109**, 022001 (2024).
[54] A. Gelman and D. B. Rubin, Stat. Sci. **7**, 457 (1992).
[55] C. Cutler and É. E. Flanagan, Phys. Rev. D **49**, 2658 (1994).
[56] L. S. Finn, Phys. Rev. D **46**, 5236 (1992).
[57] P. Schmidt, I. W. Harry, and H. P. Pfeiffer, arXiv:1703.01076.
[58] M. Ruiz, R. Takahashi, M. Alcubierre, and D. Nunez, Gen. Relativ. Gravit. **40**, 2467 (2008).
[59] P. Schmidt, M. Hannam, S. Husa, and P. Ajith, Phys. Rev. D **84**, 024046 (2011).
[60] E. Baird, S. Fairhurst, M. Hannam, and P. Murphy, Phys. Rev. D **87**, 024035 (2013).
[61] P. Schmidt, F. Ohme, and M. Hannam, Phys. Rev. D **91**, 024043 (2015).
[62] C. Hoy, Phys. Rev. D **106**, 083003 (2022).
[63] A. Ramos-Buades, A. Buonanno, H. Estellés, M. Khalil, D. P. Mihaylov, S. Ossokine, L. Pompili, and M. Shiferaw, Phys. Rev. D **108**, 124037 (2023).
[64] J. E. Thompson, E. Hamilton, L. London, S. Ghosh, P. Kolitsidou, C. Hoy, and M. Hannam, Phys. Rev. D **109** 063012 (2024).
[65] J. D. Hunter, Comput. Sci. Eng. **9**, 90 (2007).
[66] C. Hoy and V. Raymond, SoftwareX **15**, 100765 (2021).
[67] C. R. Harris *et al.*, Nature (London) **585**, 357 (2020).
[68] P. Virtanen *et al.* (SciPy 1.0 Contributors), Nat. Methods **17**, 261 (2020).